

Power-law intensity distribution in γ -decay cascades

Keisuke Fujii^{1,2,*} and J. C. Berengut^{3,2}

¹*Department of Mechanical Engineering and Science,*

Graduate School of Engineering, Kyoto University Kyoto 615-8540, Japan

²*Max-Planck-Institut für Kernphysik, Saupfercheckweg 1, 69117 Heidelberg, Germany*

³*School of Physics, University of New South Wales, New South Wales 2052, Australia*

(Dated: March 14, 2022)

We show that the distribution of γ -decay intensities from heavy nuclei follows a power law. This is similar to the long-reported result that the distribution of electromagnetic emission line intensity from many-electron atoms follows a power law, however we find that in heavy nuclei the distribution always has a specific index 1, i.e., Zipf's law. This phenomenon is observed all 27 data sets having sufficient γ -ray intensity entries in the National Nuclear Data Center database, regardless of the reaction type or nuclei involved. This agreement can be understood from combining two statistical models: exponentially increasing level density, and independently distributed line strengths among all the excited states. We also present a joint probability distribution of the γ -ray energy and intensity, which may be used to estimate the gamma strength function for highly excited nuclei.

The line intensity distribution for many-electron atoms (one of the most well-studied fermionic many-body systems) in plasmas has been reported to exhibit a power law dependence [1–4],

$$\rho_I(I) \propto I^{-c-1}, \quad (1)$$

where $\rho_I(I)$ is the number of emission lines having intensity I and c is the index of the power law. In our earlier work [5], we have shown that the index can be written as $c = kT_e/\epsilon_0$, where k is the Boltzmann's constant, T_e is the electron temperature in the plasma, and ϵ_0 is an atom-dependent constant related to the level density of the atom (as we see later). This relation is derived based on statistical properties commonly seen also in other fermionic many-body systems, namely the exponentially increasing level density and independently distributed transition rates among excited states. A similar law is expected for other systems, e.g., heavy nuclei, although to our knowledge no studies have been reported.

In this Letter, we show that the intensity distribution of the electromagnetic emission lines from excited nuclei, i.e., γ -decay spectra, also follows a power law. However, in the nuclear case the exponent has the specific index 1 (Zipf's law), i.e., $\rho_I(I) \propto I^{-2}$. We show that this result can be derived based on those same statistical properties of many-body fermionic systems that lead to the power law in atomic systems. The key difference, leading to the different exponents, is that the nuclear excitations are a result of nuclear reactions that populate only a few highly-excited states, while the atomic excitations result from processes that excite a thermal distribution states. Experimentally observed γ -decay spectra for many types of nuclear reactions are found to follow Zipf's law, regardless of the nuclei and the type of reactions. This observation suggests that the power-law distribution of

the electromagnetic emission intensity is a generic property of fermionic many-body systems.

To derive the intensity distribution, we model the joint probability distribution of the intensity and energy of γ -rays, which is found to depend on the gamma strength function between highly excited states through its γ -ray energy dependence. Although the Oslo-method has been used to estimate this function [6–8], and to validate the Brink-Axel hypothesis [8–10], cross validation with another method is still important. Our joint distribution may be also be used for this purpose.

Let us start from the level density of a nucleus $\rho_E(E)$, i.e., the number of levels with a given excited energy E . In general, $\rho(E)$ shows a nearly exponential dependence on E . One simple yet well-accepted approximation is the constant temperature model [12],

$$\rho_E(E) \propto \exp\left(\frac{E}{\epsilon_0}\right), \quad (2)$$

where ϵ_0 parameterizes the level-density growth rate with excited energy (called *temperature* in Refs. [12, 13]).

After typical nuclear reactions, such as thermal neutron capture, a few of the highly excited states (with energy E_{\max}) become populated. These excited nuclei spontaneously decay to the lower levels by emitting γ -rays (γ -decay). This decay process continues until the nuclei reach the ground state. Figure 1 (a) shows an illustration of the cascading process for a typical example: the neutron capture on ^{89}Y .

Consider an ensemble of nuclei undergoing the nuclear reaction. The population n_i of a state i with excitation energy $E_i < E_{\max}$ is determined by this cascading process. Let A_{ij} be the spontaneous transition rate from state i to state j . The rate equation of the population n_i is

$$\frac{dn_i}{dt} = \sum_{j>i} A_{ji}n_j - \sum_{j<i} A_{ij}n_i, \quad (3)$$

where $\sum_{j>i}$ ($\sum_{j<i}$) denotes a summation for all the states j that have higher (lower) energy than E_i . The

* fujii@me.kyoto-u.ac.jp

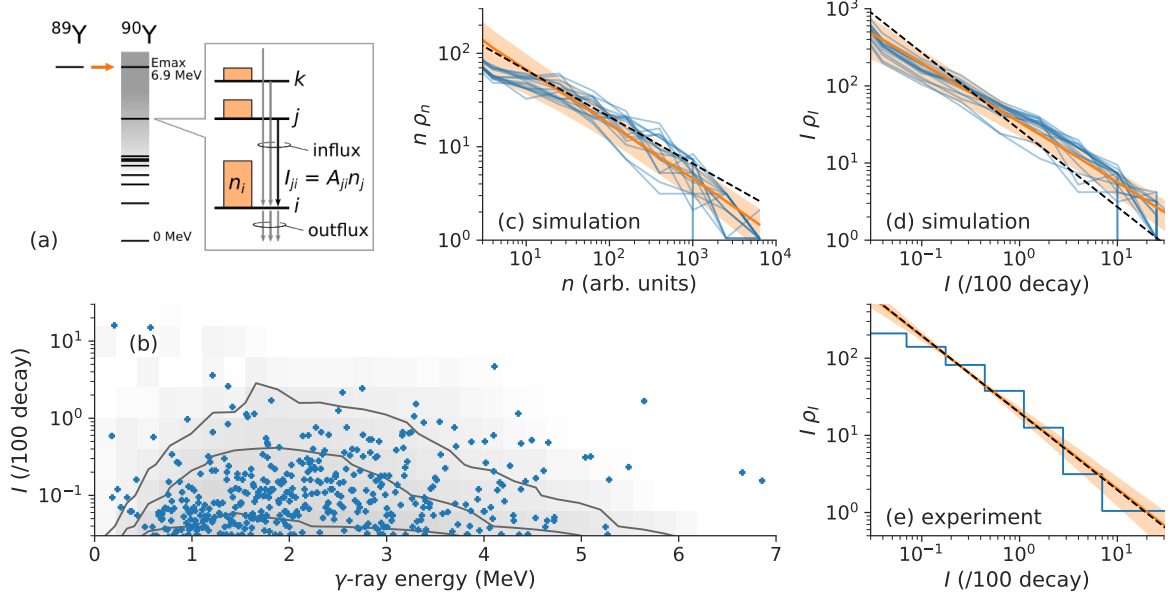


FIG. 1. γ -decay cascade of ^{90}Y after neutron capture by ^{89}Y . (a) Schematic illustration of the cascade. The direct population influx is at the $E_{\text{max}} = 6.9$ MeV level, and the excited ^{90}Y nucleus decays to lower levels. The population in each level is determined by the balance between the population influxes from higher levels and outfluxes to the lower ones. (b) Joint distribution of γ -ray intensity and energy. The contours are computed using **RAINIER** while markers show the entries in the ENSDF database [11]. (c) Population distribution ρ_n and (d) intensity distribution ρ_I simulated using the **RAINIER** program. Each blue line shows a computed result by the program, with different random number realizations. Solid straight lines show the maximum-likelihood estimates for these results with bands indicating 2σ -uncertainty. Dotted lines show our model predictions (Eqs. (10) and (12), respectively). Note that the vertical axes are multiplied by n and I , respectively, to aid visualization. (e) Intensity histogram of observed γ -rays from the ENSDF database [11]. The maximum-likelihood estimate and its 2σ range are shown by a straight line and bands, respectively. Our prediction (Eq. (12)) is shown by a dotted line.

first term in the right-hand side represents the population influx to state i from higher levels, while the second term denotes the population outflux to the lower levels.

We now utilize another stochastic property of many-body quantum chaotic systems [14] — that line strengths S_{ij} are independent and randomly distributed. For electric-dipole transitions $A_{ij} \propto \omega_{ij}^3 S_{ij}$ with $\omega_{ij} = E_i - E_j$. A typical approximation that has been used for heavy nuclei transitions is the Porter-Thomas distribution, $p_S(S_{ij}|\omega_{ij}) = \frac{1}{\sqrt{2\pi S_{ij} \bar{S}(\omega_{ij})}} \exp\left(-\frac{S_{ij}}{2\bar{S}(\omega_{ij})}\right)$, where $\bar{S}(\omega_{ij}) = 2\pi\Gamma(\omega_{ij})$ is the average line strength, with $\Gamma(\omega_{ij})$ the gamma strength function, which has been often assumed as transition-energy dependent but state independent [8–10, 15–17].

Due to the high density of many-body excited states, we may approximate the summations in Eq. (3) by integrals, taking Eq. (2) into account. The continuous rate equation may be written as

$$\begin{aligned} \frac{dn(E)}{dt} &\propto \int_0^{E_{\text{max}}-E} \omega^3 \bar{S}(\omega) \rho(E+\omega) n(E+\omega) d\omega \\ &\quad - \int_0^E \omega^3 \bar{S}(\omega) \rho(E-\omega) n(E) d\omega, \end{aligned} \quad (4)$$

where we use the average of S under the assumption that S is independently distributed and the existence of many

cascading channels ensures that fluctuations in S are cancelled out. $n(E_i)$ is the population of the state i , and so $n(E+\omega)\rho(E+\omega)d\omega$ is the population in the states within the energy range of $E+\omega \sim E+\omega+d\omega$. As the γ -decay rate is much faster than the experimental time scale, we consider the steady state for $n(E_i > 0)$:

$$\begin{aligned} \exp\left(\frac{E}{\epsilon_0}\right) \int_0^{E_{\text{max}}-E} \omega^3 \bar{S}(\omega) \exp\left(\frac{\omega}{\epsilon_0}\right) n(E+\omega) d\omega \\ = \exp\left(\frac{E}{\epsilon_0}\right) \int_0^E \omega^3 \bar{S}(\omega) \exp\left(-\frac{\omega}{\epsilon_0}\right) n(E) d\omega. \end{aligned} \quad (5)$$

Although Eq. (5) is not analytically solvable, we may adopt a further simplification. As seen in Fig. 1 (b), most of the γ -lines fall into $\omega \ll E_{\text{max}}$ region. This suggests that the value of the integrands on both sides of Eq. (5) are small for large ω . Therefore, neglecting edge effects, we can expand the limits of integration to

$$\int_0^{E_{\text{max}}-E} \cdot d\omega \approx \int_0^\infty \cdot d\omega, \quad \int_0^E \cdot d\omega \approx \int_0^\infty \cdot d\omega. \quad (6)$$

With this approximation, Eq. (5) becomes translation invariant, i.e. $n(E) \propto n(E+\Delta)$ for all E . Thus, the solution has the form $n(E) \propto \exp(-\alpha E)$ with a constant α . By substituting this into Eq. (5) with the infinite-integration-range approximation, the population $n(E)$ is

deduced as

$$n(E) \propto \exp\left(-\frac{E}{\epsilon_0/2}\right). \quad (7)$$

Alternatively, this may be considered as the distribution of probability that a level takes part in the cascade.

Let us count the number of states having population $n \sim n + dn$. This can be deduced by substituting Eq. (7) into Eq. (2),

$$\begin{aligned} \rho_n(n)dn &= \rho_E(E)dE \\ &\propto \rho_E(E)\frac{1}{n}dn \\ &\propto n^{-3/2}dn. \end{aligned} \quad (8)$$

A power law thus emerges for the state population distribution. This power law originates from the combination of one exponentially increasing variable and another exponentially decreasing variable. This is a typical mathematical structure responsible for the emergence of the power law [18].

Neglecting the stochastic nature of S , the intensity of γ -rays having photon energy ω and upper state energy E can be written as

$$I(E, \omega) \propto \omega^3 \bar{S}(\omega)n(E), \quad (9)$$

where E is the upper level energy. See the supplemental material of Ref. [5] for a more detailed and precise discussion of this approximation.

Now consider the number of emission lines having γ -ray energy $\omega \sim \omega + d\omega$ from the excited states existing within $E \sim E + dE$. The number of lines may be approximated by the number of levels in the corresponding energy range,

$$\begin{aligned} L(E, \omega)dE d\omega &= \rho_E(E - \omega)d\omega \rho_E(E)dE \\ &\propto \exp\left(\frac{2E}{\epsilon_0}\right) \exp\left(-\frac{\omega}{\epsilon_0}\right) d\omega dE. \end{aligned} \quad (10)$$

By substituting Eq. (9) into Eq. (10), the number of lines whose intensities and photon energies are in the range $I \sim I + dI$ and $\omega \sim \omega + d\omega$, respectively, i.e., a joint distribution of γ -rays, is given by

$$\begin{aligned} \rho_I(I, \omega)dI d\omega &= L(E, \omega)dE d\omega \\ &\propto L(E, \omega)I^{-1}dI d\omega \\ &\propto \omega^3 \bar{S}(\omega) \exp\left(-\frac{\omega}{\epsilon_0}\right) I^{-2}dI d\omega. \end{aligned} \quad (11)$$

Integrating Eq. (11) in the measured energy range Ω over ω , we arrive at Zipf's law for the γ -ray intensity:

$$\rho_I(I) = \int_{\Omega} \rho_I(I, \omega)d\omega \propto I^{-2}. \quad (12)$$

Note that there is no Ω dependence in the exponent as long as $\omega \ll E_{\max}$ is satisfied.

We compare the above model with a numerical simulation as well as the experimentally observed γ -ray emissions following the ^{89}Y neutron capture process.

RAINIER is a simulation tool for distributions of excited nuclear states and cascade fluctuations [19]. This adopts more exact nuclear properties, e.g., the back shifted Fermi gas model is used for the level density, taking into account parity and angular momentum distributions, some known low-lying energy levels, and the generalized Lorentzian form for the gamma strength function.

For our simulation, the level density parameters and gamma strength function parameters are taken from Ref. [13] and Ref. [20], respectively. Since the levels and the line strengths in RAINIER are constructed in a random manner, we carry out the computations 100 times with different random number realizations. The contour in Fig. 1 (b) shows the joint distribution function of γ -ray intensity and energy. This qualitatively agrees with the observations (markers) taken from ENSDF database [11].

Figure 1 (c) and (d) show $\rho_n(n)$ and $\rho_I(I)$, respectively, obtained using RAINIER. Multiple kinked-lines in the figures show 16 samples with different realizations. Despite the drastic approximations made in this work, our prediction (Eq. (8) and Eq. (12), dotted lines in the figure) reproduces these distributions well.

We fit the simulated distribution with the following power law functions:

$$\rho_n(n) \propto n^{-c'-1} \quad (13)$$

$$\rho_I(I) \propto I^{-c-1} \quad (14)$$

where c' and c are adjustable parameters to be estimated by the maximum-likelihood method. The extracted values are $c' = 0.61 \pm 0.05$ and $c = 0.78 \pm 0.04$, respectively. These values are close to our model predictions, $c' = 1/2$ and $c = 1$.

Figure 1 (e) shows ρ_I for the experimentally observed γ -ray intensities in this process, computed from the intensities registered in ENSDF database [11]. The distribution also reproduces a power-law behavior well, except at low intensities where it is possible that the data is incomplete, e.g., some of the weak lines could be indistinguishable from noise or continuum. We also fit this data by Eq. (14) for intensities with $I > 0.1$ (/100 decays). The maximum-likelihood estimate gives $c = 0.96 \pm 0.07$, in agreement with our theoretical prediction, $c = 1$ (Eq. (12)).

We have repeated a similar analysis for other nuclei and reactions using the γ -ray intensity data from ENSDF database [11]. We analyzed the 27 reactions that have more than 100 γ -ray entries with intensities larger than the minimum detection limit of the continuum. The analyzed reactions can be found in the vertical axis of Fig. 2. Figure 2 (a) shows the values of ϵ_0 by Egidy *et al.* [13], while the estimated c values for these data are shown in Fig. 2 (b). Although ϵ_0 has a negative dependence on nuclei mass A ($\approx A^{-2/3}$ [13]) and varies by a factor 5 in this range, c is distributed in the range 1.03 ± 0.15 . This

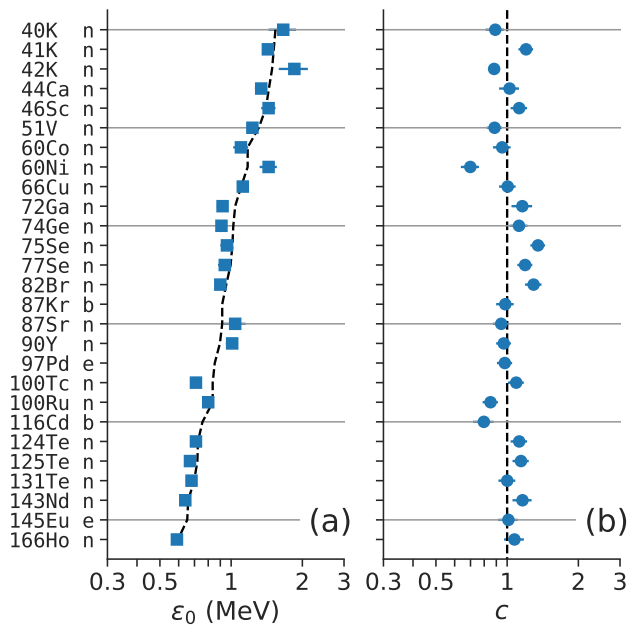


FIG. 2. (a) Values of ϵ_0 for several cascading nuclei [13]. ‘n’, ‘b’, and ‘e’ in the vertical axis represent the reaction type, thermal neutron capture, β -decay, and electron capture, respectively. For example, ‘ ^{90}Y n’ indicates γ -rays from ^{90}Y generated by thermal neutron capture. The dashed line shows $A^{-2/3}$ where A indicates the nuclear mass number. (b) Values of the exponent c from the intensity distribution power-law estimated by the maximum-likelihood method for several nuclear reactions. ϵ_0 varies by a factor of 5 but the exponent is distributed around 1, independent of the cascading nucleus and reaction type.

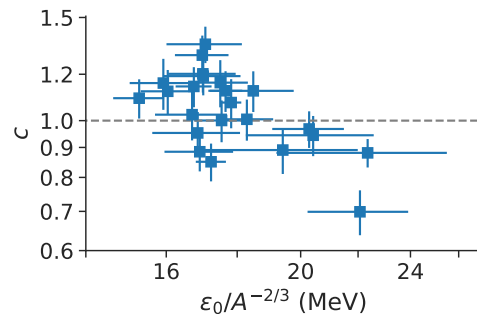


FIG. 3. Intensity distribution power-law exponent c and the level density parameter ϵ_0 scaled by $A^{-2/3}$.

indicates the generality of our model Eq. (12).

A small correlation can be seen between the scatter of ϵ_0 and c in Fig. 2. For example, ^{60}Ni has higher ϵ_0 value than the $A^{-2/3}$ trend, while its exponent has smaller value than 1. In Fig. 3, we show a scatter plot between the exponent c and the level density parameter ϵ_0 scaled by $A^{-2/3}$. They show a negative correlation. This suggests some information about the nuclear structure is contained in the intensity histogram. However, in the current stage of the analysis, this correlation is still an open question and left for a future study.

In this Letter, we showed from a coarse approximation of the population dynamics in nuclei that γ -ray intensities from nuclear reactions follow Zipf’s law with index 1. As can be found in Eq. (11), we derived the joint distribution of the γ -ray frequency and intensity. Although we only discussed the marginal distribution Eq. (12) in this work, the joint distribution Eq. (11) has information about the gamma strength function. This distribution may be used to estimate and validate the gamma strength function between highly excited states, which is an indispensable quantity to estimate stellar reaction rates relevant for nucleosynthesis [21–23]. Note that, however, due to the approximation Eq. (6), the population model Eq. (7) is not valid at reaction energy limit ($E \approx E_{\text{max}}$). The discrepancy in the low n side of Fig. 1(c) may reflect this accuracy limitation. Therefore, a more precise treatment of Eq. (4) may be necessary to quantitatively estimate the gamma strength function from experimental spectra.

ACKNOWLEDGMENTS

This work was partly supported by JSPS KAKENHI Grant Number 19K14680, the grant of Joint Research by the National Institutes of Natural Sciences (NINS) (NINS program no. 01111905), and partly by the Max-Planck Society for the Advancement of Science. JCB is supported by the Alexander von Humboldt Foundation. We thank José Crespo López-Urrutia, Wenjia Huang, and Hans Arwed Weidenmüller, for the useful discussions.

-
- [1] R. C. M. Learner, *Journal of Physics B: Atomic and Molecular Physics* **15**, L891 (1982).
- [2] C. Bauche-Arnoult and J. Bauche, *Journal of Quantitative Spectroscopy and Radiative Transfer* **58**, 441 (1997).
- [3] J. Bauche, C. Bauche-Arnoult, and O. Peyrusse, *Atomic Properties in Hot Plasmas* (Springer International Publishing, Cham, 2015).
- [4] J.-C. Pain, *High Energy Density Physics* **9**, 392 (2013).
- [5] K. Fujii and J. C. Berengut, *Physical Review Letters* **124**, 185002 (2020).
- [6] J. Rekstad, A. Henriquez, F. Ingebretsen, G. Midtun, B. Skaali, R. Øyan, J. Wikne, T. Engeland, T. F. Thorsteinsen, E. Hammaren, and E. Liukkonen, *Physica Scripta* **T5**, 45 (1983).
- [7] A. C. Larsen, M. Guttormsen, M. Krtička, E. Běták, A. Bürger, A. Görgen, H. T. Nyhus, J. Rekstad, A. Schiller, S. Siem, H. K. Toft, G. M. Tveten, A. V. Voinov, and K. Wikan, *Physical Review C* **83**, 034315 (2011).
- [8] M. Guttormsen, A. C. Larsen, A. Görgen, T. Renstrøm, S. Siem, T. G. Torny, and G. M. Tveten, *Physical Review Letters* **116**, 012502 (2016).
- [9] D. M. Brink, *Some aspects of the interaction of light with matter*, Ph.D. thesis, University of Oxford (1955).
- [10] P. Axel, *Physical Review* **126**, 671 (1962).
- [11] “ENSDF database,” <http://www.nndc.bnl.gov/ensarchivals/>, [Accessed: 4-Sep-2019].
- [12] T. Von Egidy, H. Schmidt, and A. Behkami, *Nuclear Physics A* **481**, 189 (1988).
- [13] T. von Egidy and D. Bucurescu, *Physical Review C* **72**, 044311 (2005).
- [14] N. Bohr, *Nature* **137**, 344 (1936).
- [15] T. A. Brody, J. Flores, J. B. French, P. A. Mello, A. Pandey, and S. S. M. Wong, *Reviews of Modern Physics* **53**, 385 (1981).
- [16] G. E. Mitchell, A. Richter, and H. A. Weidenmüller, *Reviews of Modern Physics* **82**, 2845 (2010).
- [17] H. A. Weidenmüller and G. E. Mitchell, *Reviews of Modern Physics* **81**, 539 (2009).
- [18] M. V. Simkin and V. P. Roychowdhury, *Physics Reports* **502**, 1 (2011).
- [19] L. Kirsch and L. Bernstein, *Nuclear Instruments and Methods in Physics Research Section A: Accelerators, Spectrometers, Detectors and Associated Equipment* **892**, 30 (2018), arXiv:1709.04006.
- [20] H. I. KIM, M. J. YI, and Y.-O. LEE, *Journal of Nuclear Science and Technology* **44**, 1117 (2007).
- [21] DOE Offices of Nuclear Physics and Advanced Scientific Computing Research, *Report of the Nuclear Physics and Related Computational Science R&D for Advanced Fuel Cycles Workshop*, Tech. Rep. (2006).
- [22] G. J. Mathews and R. A. Ward, *Reports on Progress in Physics* **48**, 1371 (1985).
- [23] C. Sneden, J. J. Cowan, and R. Gallino, *Annual Review of Astronomy and Astrophysics* **46**, 241 (2008).